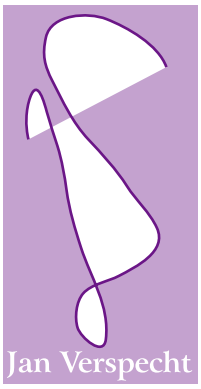

Jan Verspecht bvba

Mechelstraat 17
B-1745 Opwijk
Belgium

email: contact@janverspecht.com
web: http://www.janverspecht.com

A Simplified Extension of X-parameters to Describe Memory Effects for Wideband Modulated Signals

Jan Verspecht, Jason Horn and David E. Root

Presented at the Spring 2010 ARFTG Conference - Anaheim, CA, USA

A Simplified Extension of X-parameters to Describe Memory Effects for Wideband Modulated Signals

Jan Verspecht*, Jason Horn** and David E. Root**

* Jan Verspecht b.v.b.a., Opwijk, Vlaams-Brabant, B-1745, Belgium
** Agilent Technologies, Inc., Santa Rosa, California, CA 95403, USA

***Abstract*— An original way is presented to model memory effects of microwave amplifiers in the case of wideband modulated signals. The approach is based on X-parameters and can be used to model hard nonlinear behavior. The model can be derived from pulsed envelope X-parameter measurements on an NVNA. The result is a quasi-static nonlinear X-parameter which depends on the probability density function of the input envelope amplitudes. The model predicts RF response to conventional wide-bandwidth communication signals that excite long-term memory effects in power amplifiers. The model is implemented in the ADS circuit envelope simulator.**

***Index Terms*—behavioral model, memory effects, frequency domain, pulsed envelope, measurements, X-parameters, NVNA**

I. Introduction

Behavioral modeling of microwave components is of great interest to the designers of amplifiers that are used in today's wireless communication infrastructure. An important problem faced by these engineers is the difficulty to characterize, describe mathematically, and simulate the nonlinear behavior of amplifiers that are stimulated by signals that have a high peak-to-average ratio and that excite the amplifier over the full operating range of instantaneous power. This is problematic for at least two reasons. Firstly, the amplifier behavior may be driven into full saturation and is as such strongly nonlinear. Secondly, the amplifier behavior shows long-term memory effects. Such memory effects are caused, among others, by time-varying operating conditions such as dynamic self-heating and bias-line modulation. These changes are induced by the input signal itself and vary at a relatively slow rate compared to the modulation speed. As a consequence the instantaneous behavior of the amplifier becomes a function not only of the instantaneous value of the input signal, but also of the past values of the input signal. This is referred to as a "long term memory effect".

An original behavioral model that can accurately handle both strongly nonlinear effects and long-term dynamic memory effects has been described in [1]. This general behavioral model is called a dynamic X-parameter model and was based on the earlier Poly-Harmonic Distortion (PHD) and X-parameter work described in [2] and [3]. One of the advantages of the dynamic X-parameter model is that the model can directly be extracted by performing a set of pulsed envelope X-parameter measurements on a modern Nonlinear Vector Network Analyzer (NVNA).

In this paper we present a highly simplified version of the abovementioned dynamic X-parameter model which is valid for a wideband modulated signal or, equivalently, a fast varying input envelope signal. Note that "fast" is to be considered relative to the time constants of the nonlinear dynamic baseband effects causing the long term memory effects like e.g. thermal, biasing or trapping effects.

II. Model Theory

As described in [1] memory effects can be introduced by making use of one or more hidden variables. The idea is that, in a system with memory, the mapping from the input signal to the output signal is no longer a function of the input signal amplitude only, but is also a function of an arbitrary number N of *a priori* unknown hidden variables, denoted $h_1(t)$, $h_2(t),\ldots,h_N(t)$. These variables represent time varying physical quantities inside the component, for example temperature, bias voltages or currents, or semiconductor trapping phenomena that influence the mapping from the input RF signal to the output signal. For simplicity we deal with a unilateral and perfectly matched device and neglect all harmonics. Extensions to multi-port devices with mismatch and harmonics will be treated elsewhere.

The time-dependent envelope of the scattered wave B(t) is given by a generic nonlinear X_{21}-parameter function of the input amplitude envelope A(t) and the time-dependent values of all relevant hidden state variables, $h_i(t)$, as described by (1).

$$B(t) = X_{21}\left(\left|A(t)\right|, h_1(t), h_2(t), ..., h_N(t)\right).\Phi(t) \qquad (1)$$

with $\Phi(t) = e^{j\phi(A(t))}$.

As described in [2] the dependence of B(t) on the phase of A(t) modeled by (1) is a good approximation for many systems and its limitation will not be considered further here.

The black-box assumption about the relationship between

the input signal A(t) and the hidden variables $h_i(t)$ is mathematically expressed as

$$\mathrm{h_i}(\mathrm{t}) = \int_0^\infty \mathrm{P_i}\left(\left|\mathrm{A}(\mathrm{t}-\mathrm{u})\right|\right)\,\mathrm{k_i}(\mathrm{u})\,\mathrm{du}\,. \tag{2}$$

Equation (2) expresses that the i[th] hidden variable is generated by a linear filter operation, characterized by its impulse response $k_i(.)$, that operates on a nonlinear function $P_i(.)$ of the input signal amplitude |A(.)|. $P_i(.)$ can be interpreted as a source term that describes how the input signal is related to the excitation of a particular hidden variable. For example, $P_i(.)$ could describe the power dissipation as a function of the input signal amplitude, whereby $h_i(.)$ is the temperature. The impulse response $k_i(.)$ describes the actual dynamics of a hidden variable, e.g. the thermal relaxation.

Consider now the simplified case where the input envelope is varying fast compared to the time constants associated with the impulse responses $k_i(.)$. If the statistical properties of the input envelope are stationary the convolution described by (2) can be approximated as follows.

$$\mathrm{h_i}(\mathrm{t}) \approx \int_0^\infty \int_0^\infty P_i(a)\,p(a)\,da\,\mathrm{k_i}(u)\,du\,, \tag{3}$$

with "a" representing the stochastic variable corresponding to the input amplitude |A(.)| and with p(a) equal to the corresponding probability density function. Equation (3) can further be simplified as follows:

$$\mathrm{h_i}(\mathrm{t}) \approx K_i(\infty)\int_0^\infty P_i(a)\,p(a)\,da\ , \tag{4}$$

with $K_i(t)$ equal to the step response corresponding to the impulse response $k_i(t)$. Note that $K_i(0)$ will be equal to zero as $K_i(t)$ always corresponds to the step response of a low-pass characteristic. Equation (4) shows that the hidden variables are no longer varying over time but have a fixed "frozen" value. This "frozen" value depends on two functions: the probability density function of the amplitude of the input envelope and the nonlinear source terms $P_i(.)$. Substitution of (4) in (1) results in

$$B(t) \approx X_{21}\left(\left|A(t)\right|, K_1(\infty)\int_0^\infty P_1(a)\,p(a)\,da, \ldots\right).\Phi(t)\ . \tag{5}$$

As mentioned in [1] the X-parameter function $X_{21}(.)$ can in many practical cases be considered to have an almost linear dependency versus the hidden variables. As the integral operator in (5) is a linear operator on close to linear arguments of $X_{21}(.)$ one can bring the integral operator outside of the function. This results in

$$B(t) \approx \left(\int_0^\infty \mathrm{X_{21}}\left(\left|A(t)\right|, K_1(\infty)\,P_1(a), \ldots\right)\,p(a)\,da\right).\Phi(t) \tag{6}$$

Regardless of the number of hidden variables, one can always define a 2-dimensional kernel function $X_{ST}(.)$ given by

$$X_{ST}(x,y) = \mathrm{X_{21}}\left(x, K_1(\infty)\,P_1(y), \ldots\right), \tag{7}$$

such that

$$B(t) \approx \left(\int_0^\infty X_{ST}\left(\left|A(t)\right|, a\right)\,p(a)\,da\right).\Phi(t)\ . \tag{8}$$

The above equation shows that the resulting behavioral model is a static nonlinear transfer characteristic that is generated by taking a weighted average of an $X_{ST}(.)$ kernel function, using the probability density function of the input amplitude p(.) as a weighting function.

III. Model Identification

A. Theory

The goal of the nonlinear model identification is to determine the $X_{ST}(.)$ kernel function by a series of experiments. This is done as follows.

Consider that one wants to find the value of $X_{ST}(A_1, A_2)$. In order to find this value one applies a constant envelope amplitude of A_2 up to time zero and one switches the value of the input envelope amplitude, at time zero, to a value A_1. The value of the output B(t) right after the switching has taken place (at time "ε") will be equal to the value $X_{ST}(A_1, A_2)$.

Indeed, using (2), one finds that, for a constant input amplitude of A_2 up to time zero (with zero phase)

$$\mathrm{h_i}(\varepsilon) = \int_0^\infty \mathrm{P_i}(A_2)\,\mathrm{k_i}(\mathrm{u})\,\mathrm{du} = \mathrm{K}_i(\infty)\,P_i(A_2), \tag{9}$$

such that, using (1)

$$B(\varepsilon) = X_{21}\left(A_1, \mathrm{K_1}(\infty)\,P_1(A_2), \ldots\right) \tag{10}$$

and finally, using (7)

$$X_{ST}(A_1, A_2) = B(\varepsilon)\,. \tag{11}$$

Repeating this pulsed RF measurement for a range of A_1 and A_2 that covers the potential operating range of the device-under-test (DUT) results in the complete knowledge of the 2 dimensional model kernel $X_{ST}(.)$.

B. Experiment

The performance of the model is tested on a ZHL-11AD+, a packaged microwave amplifier from Mini-Circuits. This device-under-test (DUT) has a specified bandwidth from 2MHz to 2GHz, a gain of 11dB and a saturated output power level of 3dBm. The carrier frequency chosen for the experiment is 1750MHz. An Agilent PNA-X with the NVNA and pulsed envelope option is used for the pulsed measurements needed for model extraction as well as for the 2-tone model verification measurements.

First, the DUT is characterized by applying an extended set of large signal input steps and by measuring the response of the DUT as soon as possible after applying the pulse. Note that each of these large signal steps differs from a classic pulse measurement in the sense that the initial signal amplitude,

before the pulse, is different from zero. This initial amplitude level corresponds to the variable A_1 in (11). The amplitude after the step corresponds to the variable A_2. For our measurements "ε" is equal to 50ns as the B-wave is measured 50ns after the application of the step. Sweeping both the A_1 and the A_2 level results in a direct measurement of the 2-dimensional kernel function $X_{ST}(.,.)$. For our specific measurement the peak amplitudes of A_1 and A_2 have been swept up to a level of 0.205V (-3.8dBm) in 18 uniform steps.
The amplitude of the measured kernel function $X_{ST}(A_1, A_2)$ for the full sweep for A_1 and for a set of 6 fixed values A_2 is illustrated in figure 1.

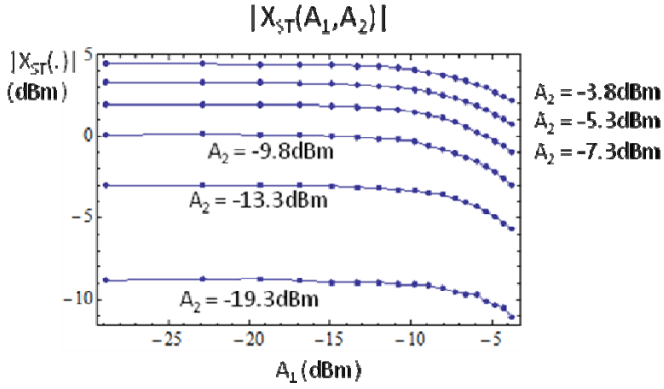

Figure 1. Amplitude of kernel function $X_{ST}(.,.)$

The phase of the measured kernel function $X_{ST}(A_1, A_2)$ for the full sweep for A_1 and for fixed value of A_2 equal to -3.8dBm is illustrated in figure 2.

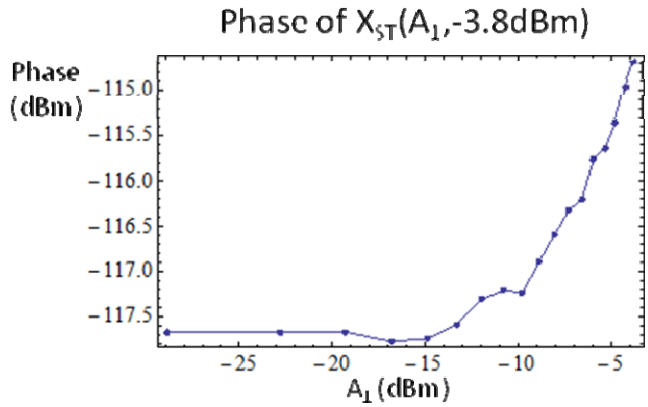

Figure 2. Phase of kernel function $X_{ST}(.,.)$

Figure 1 and figure 2 show that the amplitude and the phase of the output does not only depend on the instantaneous input amplitude A_2 but also on the value of the initial input amplitude A_1 (the input amplitude prior to the application of A_2). As can be seen in figure 1, a high initial value of A_1 causes a significant compression of the gain, even for low level instantaneous inputs. In other words, the overall gain is significantly lower right after it has been saturated.

IV. Model Verification

Once the 2-dimensional kernel $X_{ST}(.)$ has been derived from pulsed RF measurements, the actual behavioral model, as given by (8), is verified by performing a set of 2-tone verification measurements. These measurements are also performed on the Agilent PNA-X. A tone spacing, noted f_{MOD}, is chosen of 3.75MHz, symmetric with respect to the RF carrier at 1750MHz. The 2-tone measurements are performed at 4 power levels, namely -20dBm, -15dm, -12dBm and -10dBm per tone. The 2-tone input signal is generated by combining the 2 PNA-X synthesizers. The instrument will apply the input signal and will actually measure the amplitude and the phase of all the relevant tones present in the input as well as in the output signal. The spectrum of the measured input signal (the A-wave) and the corresponding output signal (the B-wave) for the highest input power level are shown in figures 3 and 4. Significant intermodulation products are present in the output signal.

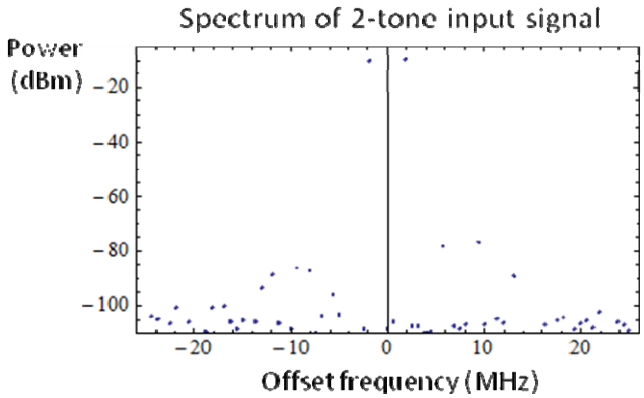

Figure 3. Measured spectrum of the 2-tone input signal

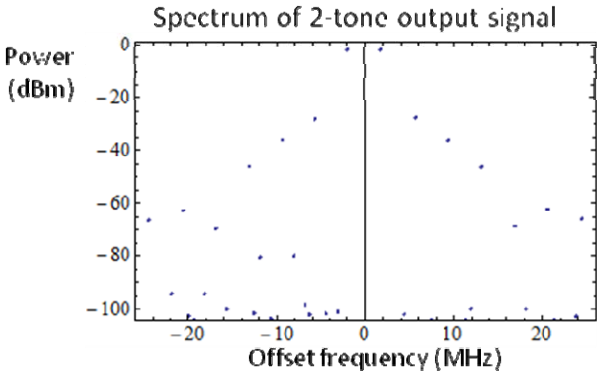

Figure 4. Measured spectrum of the 2-tone output signal

As the model expressed by (8) operates in the envelope domain, any 2-tone input signal is first to be expressed as a complex envelope. For a peak amplitude of one of the tones equal to "A", the input envelope representation A(t) is given by

$$A(t) = 2A\cos(\pi f_{MOD} t). \quad (12)$$

The envelope representation of the measured 2-tone input signal for the highest input power level is represented in figure 5, which is consistent with (12).

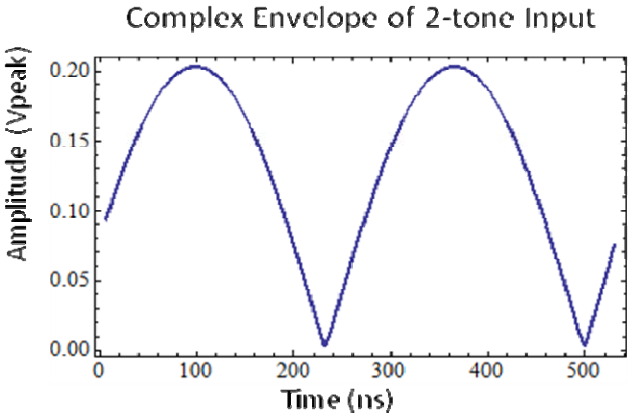

Figure 5. Complex envelope representation of 2-tone input

Equation (8) is then used to calculate the output envelopes that correspond to the given input envelope A(t). For a practical implementation the integral of (8) is approximated by a weighted average over one period of a uniformly sampled version of the periodic input envelope. For N samples, and with A[i] representing the i^{th} sample, one can calculate a sampled version of the modeled output envelope $B_{MOD}[i]$ as follows:

$$B_{MOD}[i] = \left(\frac{1}{N} \sum_{j=1}^{N} X_{ST}\left(|A[j]|, |A[i]| \right) \right) e^{j\varphi(A[i])} \quad (13)$$

The uniformly sampled modeled complex envelope $B_{MOD}[i]$ can then be compared with the uniformly sampled measured output envelope $B_{MEAS}[i]$. To highlight the performance of the new model, the result of using a traditional static compression and AM-PM characteristic (represented by the traditional static X_{21} parameter) is also calculated. The corresponding output is called $B_{SS}[i]$, it is simply calculated as

$$B_{SS}[i] = X_{21}\left(|A[i]| \right) e^{j\varphi(A[i])}. \quad (14)$$

The resulting output envelopes for the highest input power are shown in figure 6. Figures 6 clearly shows that the complex envelopes as calculated by using the new model are much more accurate than the envelopes that are calculated by using the static X_{21} parameter (which is equivalent to a traditional compression and AM-PM characteristic).

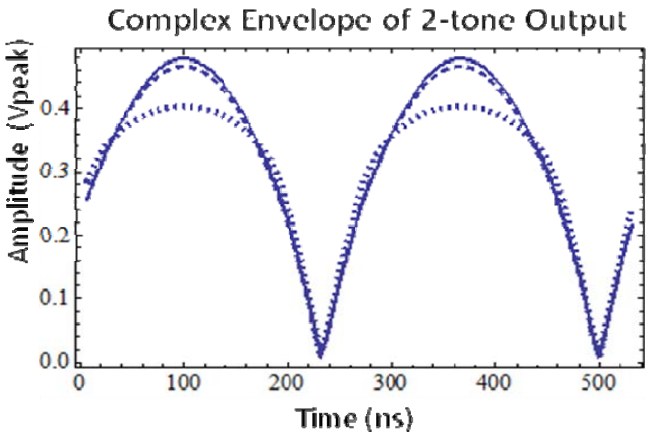

Figure 6. Amplitude of output envelope for highest input power (B_{MEAS}= solid, B_{MOD} = dashed, B_{SS} = dotted)

Using a discrete Fourier transform on the modeled output envelopes results in the modeled spectra. This allows to verify the capability of the model to predict 2-tone compression characteristics and intermodulation products. The modeled 2-tone compression characteristic and IM3-products are shown in figures 8 and 9. These figures clearly show that the new model can predict the 2-tone compression characteristic and the IM3 products with great accuracy and as such outperforms a traditional static compression and AM-PM characteristic.
Tables 1 to 3 contain the measured and modeled 2-tone gain, IM3 products and IM5 products for the 4 input power levels.

Table 1. Comparison of measured and modeled gain

Input power (dBm per tone)	-20	-15	-12	-10
Measured gain (dB)	10.41	9.84	8.85	7.97
Stochastic model gain (dB)	10.39	9.71	8.60	7.65
Static model gain (dB)	10.35	9.52	8.19	7.07

Table 2. Comparison of measured and modeled IM3

Input pow. (dBm per tone)	-20	-15	-12	-10
Measured IM3 (dBm)	-53.0	-35.5	-28.9	-28.0
Stoch. model IM3 (dBm)	-52.4	-35.1	-28.5	-27.2
Static model IM3 (dBm)	-48.0	-31.0	-23.1	-20.1

Table 3. Comparison of measured and modeled IM5

Input pow. (dBm per tone)	-20	-15	-12	-10
Measured IM5 (dBm)	-82.0	-68.4	-42.8	-36.1
Stoch. model IM5 (dBm)	-71.2	-67.5	-42.8	-36.9
Static model IM5 (dBm)	-67.4	-53.8	-44.0	-33.5

Except for the lowest power level IM5 product, which is near the noise floor of our measurements, the new stochastic model predicts gain, IM3 and IM5 products with an error smaller than 1dB, the errors of the static model are significantly higher.

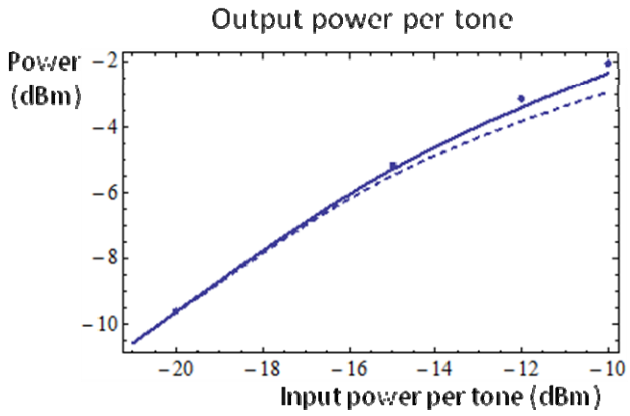

Figure 8. 2-tone compression characteristic
(measured = dots, new model= solid, static model = dashed)

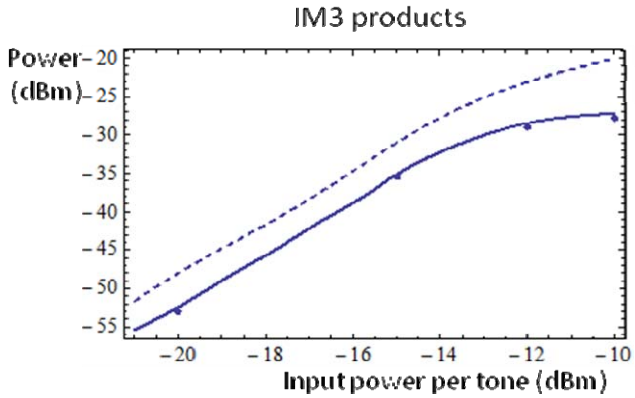

Figure 8. IM3 products
(measured = dots, new model= solid, static model = dashed)

V. Conclusions

The new behavioral model can accurately predict the nonlinear behavior like compression and intermodulation product generation of an amplifier under fast modulated conditions. The model is based on a complex envelope representation and can relatively easily be derived by performing a set of pulsed RF measurements on an Agilent PNA-X with the NVNA option.

The new model was verified using a PNA-X by performing 2-tone measurements and was shown to outperform a traditional approach based on a static compression and AM-PM characteristic.

References

[1] J. Verspecht et al.,"Extension of X-parameters to Include Long-Term Dynamic Memory Effects," *Conference Record of the IEEE Microwave Theory and Techniques Symposium 2009*, pp.601-604, USA, June 2009.

[2] J. Verspecht, D. Gunyan, J. Horn, J. Xu, A. Cognata, D. Root, "Multi-port, and Dynamic Memory Enhancements to PHD Nonlinear Behavioral Models from Large-signal Measurements and Simulations", *Conference Record of the IEEE Microwave Theory and Techniques Symposium 2007*, pp.969-972, USA, June 2007.

[3] J. Verspecht and D. Root, "Polyharmonic Distortion Modeling," *IEEE Microwave Magazine*, vol. 7, no. 3, pp. 44-57, June 2006.